

Title: Design and development of a low-cost divided bar apparatus

Authors: 1. Turlough McGuinness BE, MEngSc, MIEI 2. Phil Hemmingway BE, PhD, MIEI 3. Mike Long BE, MEngSc, PhD, CEng, MIEI, MICE

Affiliation: 1: Geotechnical Engineer, Western Australia (formerly School of Civil, Structural & Environmental Engineering, University College Dublin, Ireland).

2: Formerly School of Civil, Structural & Environmental Engineering & School of Biosystems Engineering, University College Dublin, Ireland.

3: Senior Lecturer, School of Civil, Structural & Environmental Engineering, University College Dublin, Ireland.

**Accepted for Publication in the ASTM Geotechnical Testing Journal on the 6th of
September 2013.**

Design and development of a low-cost divided bar apparatus

A divided bar apparatus is deemed to be the most accurate method of measuring the thermal conductivity, λ , (W/mK) of intact rock cores in the laboratory. The divided bar is a steady-state comparative method in which the temperature drop across a disk of rock is compared with that across a disk of standard material of known conductivity. Thermal conductivity test results obtained from rock cores can be used in software programs to determine the design requirements for any medium to large-scale ground-source energy system. This paper describes the design and development of a low-cost divided bar apparatus and compares the values obtained to those achieved by previous researchers and those recommended by EED, a commonly used borehole heat exchanger design software program. The divided bar was designed in accordance with the following principles: keep construction costs low by using readily available materials, develop a simplistic operating procedure to promote continuity of use and cater for the testing of different sized rock cores. As there are currently no recognised testing standards available for operation of a divided bar apparatus, the *sample preparation procedure for samples tested on the UCD divided bar apparatus* was developed as a proposed standard testing procedure. The proposed procedure amalgamates the developments and suggestions of previous researchers in addition to published test procedures in Ulusay and Hudson (2007), and could possibly contribute towards the development of a standardised procedure for testing on a divided bar apparatus. The test results presented in this paper demonstrate a strong relationship between thermal conductivity and mineral composition with the effects of porosity also having a notable influence on the thermal conductivity of the tested rocks.

1. Introduction

Subsurface geothermal resources represent a great potential of directly usable energy, which involves the extraction or reinjection of heat energy from or into the ground. Ground energy systems such as borehole heat exchangers are one of the best methods of harnessing this geothermal energy. A borehole heat exchanger is a ground heat exchanger devised for the extraction or injection of thermal energy from/into the ground, comprised essentially of a U-pipe within a borehole together with a heat pump. In order for a geothermal energy system to be feasible a thermal

recharge of the ground is necessary which is dependent on the ground properties. One of the most challenging aspects facing engineers designing such systems is an accurate appraisal of the grounds thermal conductivity, which in essence characterises the behaviour of these energy systems. The most accurate method of determining the in-situ value of thermal conductivity involves the execution of an in-situ thermal response test (TRT), (Hemmingway and Long, 2012a) which essentially pumps heated water through a U-pipe within a borehole and analyses the amount of heat absorption. However drilling a borehole can prove to be a costly exercise, and in the event of there being available rock cores from an adjacent borehole, it would be substantially cheaper to test the rock cores in the laboratory. The most accurate method of measuring the thermal conductivity of rock cores involves the use of a device called a divided bar apparatus.

2. The first divided bar apparatus

The divided bar is a steady-state comparative method in which the temperature drop across a disk of saturated rock is compared with that across a disk of standard material of known conductivity (Popov et al., 1999). Thermal conductivity of the rock sample is determined by comparing the temperature difference across the sample with the temperature differences across each side of the standard material (Issler and Jessop, 2011b). In theory and by design, it is a one-dimensional method to determine thermal conductivity parallel to the divided-bar axis. The divided bar method is probably the most practical method of testing thermal conductivity of rocks in the laboratory with a few different variations of the initial 'cut bar' design developed by Birch and Clark (1940). This initial design was developed by Sibbitt et al. in 1979 (Figure 1) with the lateral arrangement of disc commonly referred to as the stack.

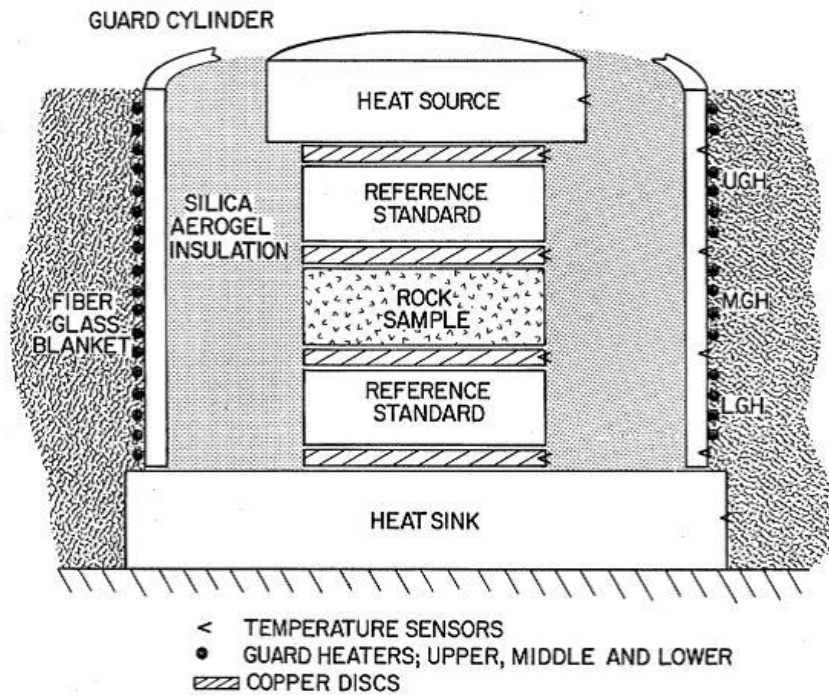


Figure 1 Schematic of cut bar thermal conductivity comparator by Sibbitt et al. (1979)

A typical divided bar exerts a retaining pressure along a cylindrical assembly in order to facilitate greater contact between adjoining surfaces and minimise contact resistance, with the pressure usually applied by hydraulic pressure or screw jack. The top and bottom of the bar is constructed so as to maintain different, but constant temperatures via heating devices, which promote a heat flux through the stack from top to bottom. The majority of heating devices to date have been comprised of water baths which allow constant temperatures to be maintained on either side of the stack arrangement.

3. UCD divided bar development

The UCD divided bar developed for testing the thermal conductivity of rock provides (i) an economical solution incorporating 'off the shelf' items (ii) an uncomplicated operating procedure within the laboratory (iii) allowance for the testing of different diameter cores. Satisfaction of these three conditions was achieved by the design and development of a divided bar apparatus, comprised of the components listed in Table 1 and presented in Figure 2.

Component	Description	Advantage
Applied Pressure	Triaxial loading machine with proving ring.	Readily available in most geotechnical laboratories. Affords the user a simplistic method of applying pressure.
Heat Source	Heating plate and controller.	Off the shelf item. Controller maintains constant temperature.
Measurement discs	Oxygen free copper	Can be purchased in solid bars. Very high thermal conductivity.
Standard discs	Polycarbonate	Inexpensive and can be purchased in various thicknesses.
Calibration Material	Fused Quartz	Consistently homogenous material with well document λ value.
Temperature Measurement	Type T thermocouple	On sale at most electronic shops and very cheap.
Insulation	Polyurethane	Flexible material which can be obtained in most hardware shops.

Table 1. UCD divided bar component selection



Figure 2 UCD divided bar apparatus

3.1 Heat source & heat sink

The heat source for the divided bar apparatus is capable of providing a constant temperature ($\pm 1^\circ\text{C}$) gradient across the cylindrical stack of materials by maintaining a constant temperature at the top and bottom of the divided bar apparatus. The majority divided bar apparatuses use temperature controlled water baths, but such an arrangement can prove difficult to construct and maintain, whereas the heaters chosen for the UCD divided bar apparatus are an 'off the shelf' item. The chosen heaters have a rated power of 118W, a maximum operating temperature of 200°C and are capable of withstanding applied pressures of up to 80N/mm^2 . The heating

controller selected allows self-optimisation of controller parameters, includes Fe-CuNi (J), NiCr-Ni (K), PT 100 DIN/IEC sensor types and operates to EN 50 082-2 and EN 50 082-1 noise immunity and emitted interference standards.

3.2 Calibration material

The divided bar apparatus was calibrated using fused quartz standard discs of different thicknesses. The discs had to be custom made for the project as such materials were not available in Ireland. The material used for the manufacture of the discs was GE124, with the discs mechanically polished to a high tolerance. Fused quartz is a noncrystalline form of silicon dioxide (SiO_2), which is also called *silica* and is comprised of silicon and oxygen with small amounts of impurities such as aluminum and titanium (Lide 2009). The thermal conductivity of fused quartz is 1.36 W/mK at 25 °C as defined in the CRC handbook (Lide, 2009).

3.3 Temperature Measurement & Electrical

The accurate measurement of temperature at precise locations is essential to the fundamental principle of heat flux through the bar, in determining the thermal conductivity of samples. This was achieved on the UCD divided bar apparatus by the use of Type T copper-constantan thermocouples embedded in the oxygen free copper measurement discs. The thermocouples are connected to a data logger allowing for the timely collection of data in addition to real time monitoring of the test.

4. Testing with the UCD divided bar apparatus

After establishment of the divided bar apparatus in the laboratory the first step was to calibrate the apparatus before testing any samples. The divided bar apparatus was calibrated using fused quartz standard discs of different thicknesses. The calibration routine is a reversal of the routine for measuring conductivity, whereby a sample of known conductivity is inserted into the divided bar, and the corresponding bar resistance is determined using Fourier's law. In order to calculate the thermal conductivity using the divided bar arrangement in the sketch, (Figure 3) three assumptions are made regarding the heat flow across the bar:-

1. Heat flow along the bar is 100% efficient with no radial heat losses. (There will always be heat loss, but insulation of the bar helps to mitigate the heat loss)
2. The reference discs are of equal thickness and thermal conductivity. This is reasonable assumption as they were machined from the same sheet of polycarbonate.
3. Finally the temperature drop across the oxygen free copper sections is assumed to be negligible compared to the temperature drop across the reference and sample sections, owing to the high thermal conductivity value.

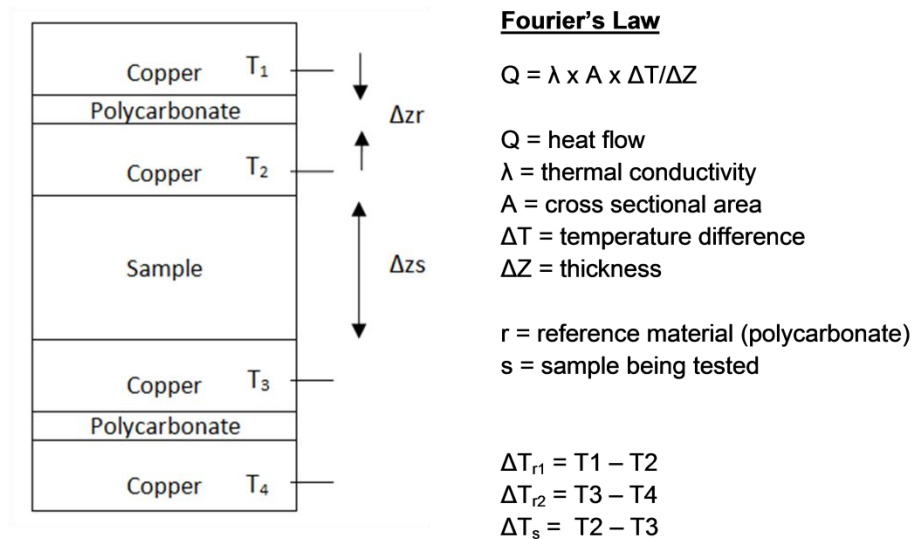


Figure 3 Schematic representation of the UCD Divided Bar Apparatus

From the first assumption, the heat flow across the bar is as follows:-

$$Q = Q_{\text{top reference disc}} = Q_{\text{sample}} = Q_{\text{bottom reference disc}}$$

$$1. Q = \lambda_r \times A_r \times \Delta T_1 / \Delta Z_r = \lambda_s \times A_s \times \Delta T_s / \Delta Z_s = \lambda_r \times A_r \times \Delta T_2 / \Delta Z_r$$

As both reference discs are equal in both size and thermal conductivity value

Equation 1 can be reworked to allow the thermal conductivity of the sample be determined as follows:

$$2. \lambda_s = \lambda_r \left[\frac{\Delta T_1 + \Delta T_2}{2 \Delta T_s} \right] \left[\frac{\Delta Z_s}{\Delta Z_r} \times \frac{A_r}{A_s} \right]$$

Equation 2 does not take into account the unwanted thermal contact resistances R , resulting from the various contacts within the bar including, heaters, copper discs and polycarbonate discs. These resistances collectively increase the apparent resistance of the sample and need to be removed when calculating the true sample thermal conductivity $\lambda_{s(\text{corrected})}$. Equation 2 can be augmented to develop $\lambda_{s(\text{corrected})}$ by removing the contact resistances R . In Equation 2 λ_r , ΔZ_r and '2' are constants in the equation, and can be grouped to give the following:

$$3. \lambda_{s(\text{measured})} = \left[\frac{\Delta T_1 + \Delta T_2}{\Delta T_s} \right] \left[\frac{A_r}{A_s} \right] \times \Delta Z_s \times C$$

$$4. \lambda_{s(\text{corrected})} = \Delta Z_s / [(\Delta Z_s / \lambda_{s(\text{measured})}) - R]$$

Substituting Equation 3 into Equation 4 gives the following:

$$5. \Delta Z_s / \lambda_{s(\text{corrected})} = \left[\frac{\Delta T_s}{\Delta T_1 + \Delta T_2} \right] \left[\frac{A_s}{A_r} \right] \times \frac{1}{C} - R$$

C and R can be determined at the same time by measuring several standard samples of known thickness and thermal conductivity such as fused quartz, with $\lambda_{s(\text{corrected})} = 1.36 \text{ W/mK}$ as reported in the CRC handbook (Lide, 2009). Two sets of tests were carried out and the results are reported on Figure 4. These trials involved testing pieces of fused quartz of 50 mm diameter and of thickness 6 mm, 9 mm and 20 mm. It can be seen that the results are repeatable and consistent and form a linear relationship with a high correlation coefficient of 0.99. The resulting "C" and "R" values are 49.505 and 0.0003 respectively. This R values is insignificant (close to zero) and will have no bearing on the subsequent results. Equation 5 is then used to determine the thermal conductivity of all test samples including the derived values of

C and R. Provided that the constituent parts of the divided bar apparatus remain unchanged and undamaged this equation can be used for all testing.

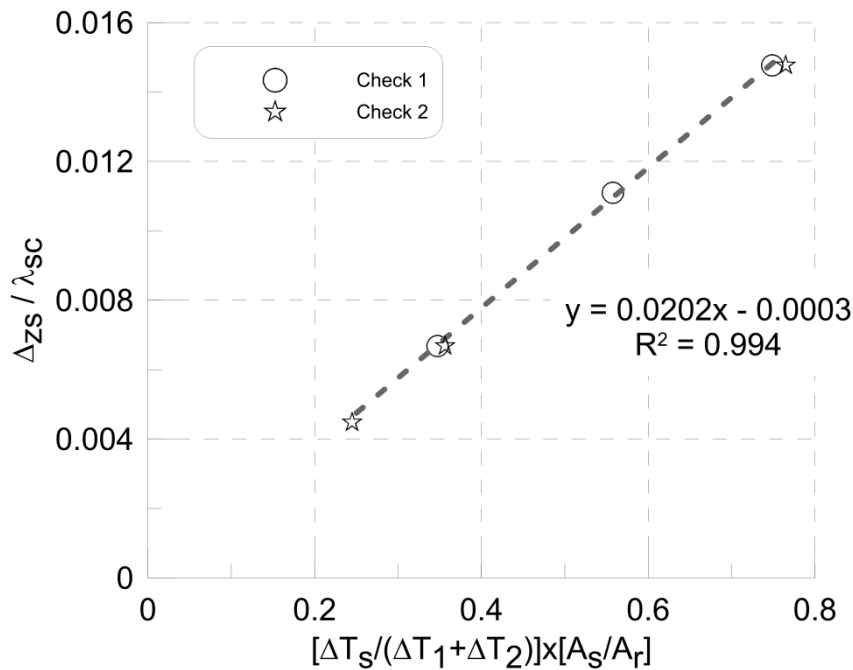


Figure 4 Straight line plot to determine C & R for the UCD divided bar apparatus

4.1 Sample Preparation

Preparation forms an integral part of testing rock samples in the divided bar apparatus and if not done correctly will yield erroneous results. The key to correct sample preparation involves producing a rock disc with parallel, flat and smooth sides fostering the maximum area of contact with the copper discs. The UCD divided bar apparatus is capable of testing samples 50 mm in diameter or smaller, however larger samples can be cored down to 50mm by means of a coring machine with a 50 mm diameter core bit. All samples were prepared in accordance with the *sample preparation procedure for samples tested on the UCD divided bar apparatus* promoting a consistent testing environment.

[Sample preparation procedure for samples tested on the UCD divided bar apparatus](#)

- i) Core and face a cylinder of rock of appropriate thickness and diameter (within 10% of the standard length and diameter and stack diameter of 50 mm). Each sample should be of sufficient length to provide three test samples.
- ii) The samples are then cut with a diamond saw perpendicular to the core axis to the required lengths ensuring that the two faces of the sample produced are parallel.
- iii) Samples are flattened by use of a flat grinding wheel, with every effort being made to ensure the faces remain parallel and not causing excessive wear to part of the face, thus promoting good thermal contacts on the divided bar equipment by avoiding wedge shapes and concave/convex surfaces.
- iv) Sample faces are then polished with Grit 400 or finer silicon carbide or diamond powder on a lap wheel to minimise thermal contact resistance, and should be flat to within ± 0.1 mm (no dome or concavity on the sample surface) and parallel to within 0.01 mm throughout (no wedge shape).
- v) Following grinding and polishing the samples are oven dried at 105°C for one week and the weight determined with an electronic balance accurate to 0.1g for porosity calculations.
- vi) Subsequently the samples are placed in a beaker full of water in a desiccator attached to a vacuum pump for 12 hours and then left to rest for another 12 hours under atmospheric pressure to allow the water fully saturate the rock.
- vii) The diameters of the samples are measured across two perpendicular diameters at mid height of the sample to the nearest 0.1 mm with a dial micrometer, whilst the height is measured at three equally spaced locations to the nearest 0.1 mm and these readings recorded with the average values reported.
- viii) The porosity, n , of the sample is calculated from Equation 6, (Ulusay and Hudson, 2007)

6. $n = 100 V_v / V$ with the pore volume, V_v calculated from Equation 7

7. $V_v / V = (\rho_s - \rho_d) / \rho_f$ where ρ_s is the saturated density, ρ_d is the dry density and ρ_f the fluid density, with the densities of the samples determined from Equation 8.

8. $\rho = M / V$ with M being the mass and V is the volume of the sample, where $V = 100 V_v / n$. (Note that the shape of samples tested and reported on in this manuscript were consistently regular cylindrical, and therefore their volume was calculated from measurements of the sample height and diameter. Volume measurement of non-regular pieces would require an alternative method, such as water displacement).

ix) All contacting surfaces are lubricated with glycerine gel prior to assembly in the divided bar apparatus to reduce any contact resistance (contact resistance can be particularly significant if air is present on the contact surfaces, or if the surfaces are rough. Application of a thin layer of high conductivity fluid ensures that contact resistances are consistent when testing varying material types (Stepanic and Milosevic, 2009)).

x) The sample is then carefully placed in the stack with great care being taken so as to ensure neither the sample or the copper discs are damaged (small imperfections on the surface of either the sample or the copper discs could result in erroneous measurements).

5. Divided bar test results

Rock core samples tested in the UCD divided bar apparatus include Calp limestone rock cores recovered from a site in Dublin along with sandstone cores received from Ardnacrusha in County Clare. Small amounts of granite and schist were tested to introduce variability in the results and clarify if the results are typical of the expected

values for the particular rock type. The depth of the borehole through Calp limestone in Dublin was 116 m, whereas the depth of the borehole in Ardnacrusha was 370 m therefore a thermal conductivity profile with depth was examined for each borehole presented here in Figure 5. The limestone samples were tested ‘as delivered’ (AD), on an oven dry basis (OD) and finally on a saturated and surface dry basis (SSD) to assess the variability of thermal conductivity with moisture content. Owing to the length of time the sandstone samples were in storage it was decided to test them on an oven dry basis (OD) and on a saturated and surface dry basis (SSD) only. The magnitude of the applied temperature drop between the source and the sink was of the order of 10-15 °C. Temperature drift in the case of both the heat source and heat sink was observed to be less than ± 0.25 °C. The test results, including details of sample extraction depth, sample diameter, sample height, bulk density, dry density and measured thermal conductivity are summarised in Table 2 (ESB Limestone) and Table 3 (ESB Sandstone).

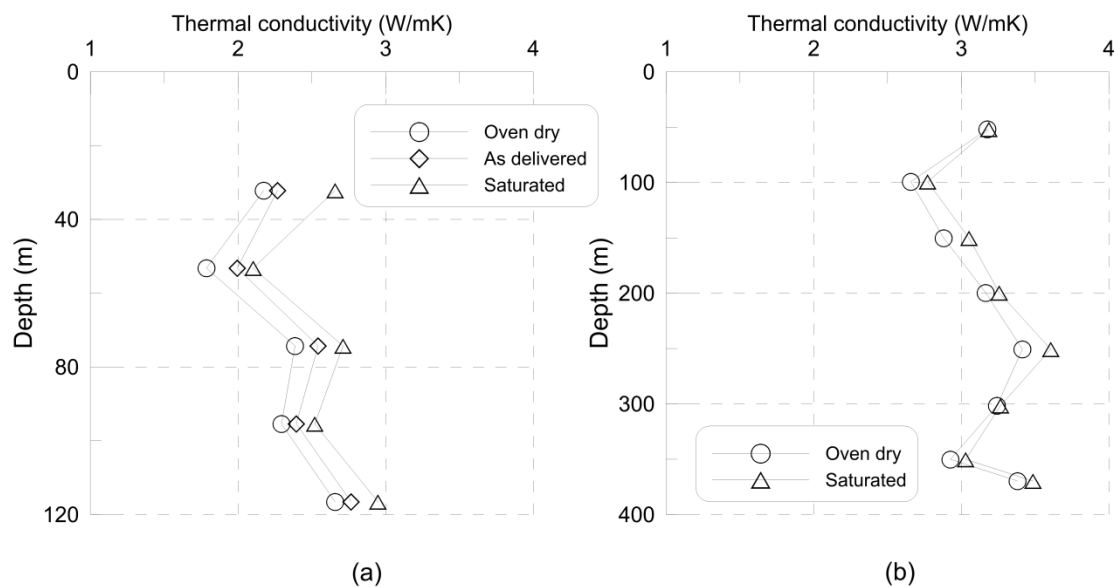


Figure 5 Thermal conductivity vs. depth for (a) Calp limestone and (b) sandstone

From Figure 5 it is apparent that no direct correlation exists between thermal conductivity and depth for either the limestone or sandstone from the depths examined as part of this study. However there is a definite trend of increasing thermal conductivity with increasing moisture content as all the samples tested display a greater value of conductivity from oven dry to being fully saturated as illustrated by the obvious gaps between the curves in Figure 5. On average the Calp limestone thermal conductivity values at the as-delivered moisture content are 92%

of the maximum values on a SSD basis, with the OD values typically achieving 87% of the SSD values. The average value of thermal conductivity for the borehole at its as delivered moisture content is 2.39 W/mK compared with 2.59 W/mK on a SSD basis. Similar to the limestone samples tested, the thermal conductivity of the sandstone was greater when the samples were saturated, but the difference was not as great owing to a smaller degree of porosity. The maximum average value of 3.61 W/mK was found at approximately 250 m b.g.l., with the thermal conductivity of the OD samples typically being 96% of the SSD samples. The average value of thermal conductivity for the borehole in its oven dry condition is 3.05 W/mK compared with 3.21 W/mK on a SSD basis.

						Thermal Conductivity (W/mK)						
Sample (m)	Dia (mm)	Height (mm)	Bulk density (kg/m ³)	Dry density (kg/m ³)	Porosity (%)	OD	Avg.	AD	Avg	S	Avg	SDev
32.0-32.3	49.6	20.5	2,703.4	2,682.5	2.09	2	2.17	2.16	2.27	2.71	2.66	0.06
	49.6	20.6	2,696.9	2,675.6	2.14	2.32		2.39		2.66		
	49.6	19.5	2,704.2	2,682.2	2.2	2.2		2.25		2.6		
53.0-53.4	49.6	20.8	2,719.3	2,691.2	2.81	1.89	1.79	2.05	1.99	2.13	2.1	0.12
	49.6	19.9	2,703.6	2,669.0	3.46	1.73		1.96		2.04		
	49.6	20.4	2,670.6	2,634.9	3.57	1.71		1.84		1.98		
	49.6	20.4	2,719.1	2,688.6	3.06	1.82		2.13		2.26		
74.0-74.52	49.6	21.1	2,579.2	2,565.0	1.42	2.13	2.39	2.26	2.54	2.52	2.71	0.26
	49.6	20.5	2,592.0	2,580.4	1.16	2.54		2.76		3		
	49.6	20.5	2,598.0	2,584.5	1.35	2.48		2.61		2.61		
95.185-95.66	49.6	21.1	2,703.6	2,684.7	1.9	2.44	2.29	2.55	2.39	2.69	2.52	0.15
	49.6	20.2	2,701.7	2,680.7	2.11	2.29		2.4		2.45		
	49.6	20.3	2,690.4	2,665.6	2.48	2.16		2.23		2.42		
116.5-116.6	49.6	20.4	2,670.1	2,667.4	0.27	2.53	2.66	2.58	2.77	2.78	2.95	0.24
	49.6	20.4	2,790.2	2,786.2	0.4	2.79		2.95		3.11		

Table 2. ESB limestone – summary of test results

						Thermal Conductivity				
Sample (m)	Dia	Height (mm)	Bulk density (kg/m3)	Dry density (kg/m3)	Porosity (%)	OD	Avg.	Saturated	Avg	SDev
51.855							3.18		3.19	0.05
1A	47.6	19.8	2728	2726	0.18	3.15		3.15		
1B	47.6	20.1	2718	2716	0.24	3.13		3.16		
1C	47.6	19.8	2692	2690	0.22	3.24		3.24		
99.303							2.66		2.77	0.12
2A	47.6	20	2747	2733	1.42	2.62		2.72		
2B	47.6	18.7	2741	2727	1.41	2.59		2.68		
2C	47.6	19.8	2758	2749	0.93	2.76		2.92		
150.115							2.88		3.05	0.2
3A	47.6	19.8	2751	2739	1.15	2.85		2.87		
3B	47.6	18.9	2759	2752	0.75	3.08		3.27		
3C	47.6	18.2	2747	2738	0.87	2.72		3.02		
196.633							3.16		3.26	0.03
4A	47.4	19.6	2724	2722	0.26	3.09		3.29		
4B	47.4	20	2719	2716	0.27	3.23		3.26		
4C	47.4	19.4	2721	2718	0.25	3.17		3.22		
250.603							3.41		3.61	0.24
5A	47.6	19	2764	2759	0.54	3.69		3.87		
5B	47.6	19.8	2791	2785	0.56	3.16		3.52		
5C	47.6	19.8	2787	2782	0.52	3.39		3.42		
301.643							3.24		3.26	0.03
6A	47.6	19.1	2722	2718	0.41	3.23		3.23		
6B	47.6	19.1	2725	2721	0.42	3.25		3.29		
6C	47.6	19.5	2754	2750	0.37	3.24		3.28		
350.108							2.93		3.03	0.08
7A	47.6	20.5	2780	2778	0.18	3.07		3.11		

7B	47.6	18.8	2757	2756	0.15	2.79		3.02		
7C	47.6	20.3	2761	2760	0.18	2.91		2.95		
369.69							3.38		3.48	0.04
8A	47.6	19.6	2699	2697	0.18	3.35		3.49		
8B	47.6	19.8	2682	2681	0.15	3.33		3.45		
8C	47.6	19.9	2691	2689	0.15	3.46		3.52		

Table 3. ESB sandstone – summary of test results

5.1 Thermal conductivity Examined with Density and Porosity

Density and porosity measurements were included as part of the sample preparation procedure for rock discs tested on the UCD divided bar apparatus. Porosity values of the Ardnacrusha sandstone are quite low, ranging from 0.15 % - 1.41 % with densities of 2680 kg/m³ to 2790 kg/m³ which is typical for sandstone rock according to Jones (2003) and Hartmann et al. (2005). The porosities of the Dublin Calp Limestone are slightly higher ranging from 0.27 % - 3.57 %, with the bulk density ranging from 2579 kg/m³ to 2790 kg/m³ as expected for Dublin limestone according to the Dublin Metro North Site Investigation Report (RPA 2008). A plot of thermal conductivity against porosity for both rock types can be seen in Figure 6.

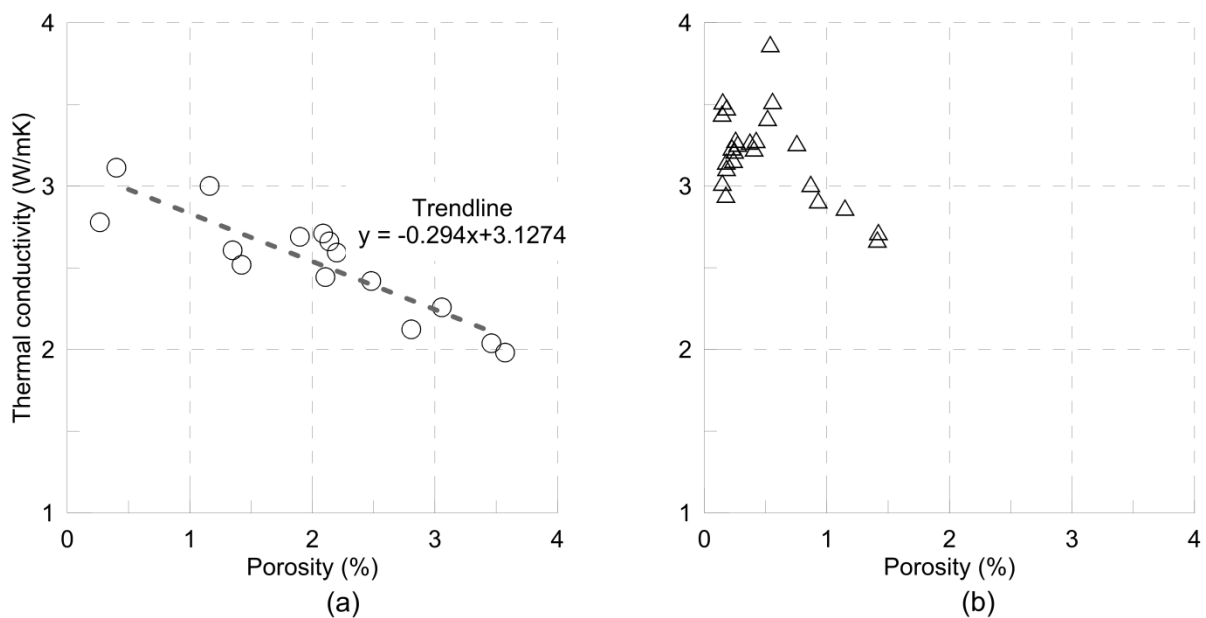


Figure 6 Thermal conductivity vs. porosity for (a) Calp limestone and (b) sandstone

In Figure 6 it is evident that a clear relationship between increasing thermal conductivity and decreasing porosity exists for the SSD Calp limestone rock, whereas the porosity versus thermal conductivity graph for the SSD sandstone rock appears to have no relationship for porosities less than 0.5%. However for the sandstone samples with a porosity of 0.5% or greater the thermal conductivity value tends to decrease with increasing porosity, in a similar fashion to the limestone. For the sandstone it can be concluded that rock with porosities of 0.5 % or less will have a negligible effect on the thermal conductivity of the rock mass and samples with a

porosity of 0.5% or greater will have a mitigating effect on the thermal conductivity value.

Figure 7a shows some available data for thermal conductivity tests on limestone compared to the data obtained as part of this study. These data include tests on limestones from Southern Germany (Pechnig et al., 2007), Turkey (Canakci et al., 2007a) and the United States (Robertson, 1988). For all the sites, the thermal conductivity at very low porosity approaches the value of 3 W/m K which is close to that of pure calcite, which has been reported to have a thermal conductivity of 3.4W/mK (Horai, 1971). In all cases the thermal conductivity then subsequently decreases with increasing porosity. The rate of decrease is greatest for the Irish limestone but this rate is not dissimilar to the results for the Turkish and German rocks.

Figure 7b presents a similar set of results for sandstones and compares against measurements made by a number of other researchers (Woodside and Messmer, 1961, Issler and Jessop, 2011a, Hartmann et al., 2005). Again the porosity is a dominant factor in the resulting thermal conductivity of the rock. The absolute value of thermal conductivity for the sandstones show more variance than those for the limestones – presumably because of the varying amount of high conductivity quartz present. The limestone and sandstone values assimilate well with the earlier part of the graph as the majority of porosity values obtained by others tend to be greater than 5 %.

The inclusion of the UCD divided bar results in Figure 7 within close proximity to results obtained by others offers a degree of confidence in the results attained here. The relationship between increasing thermal conductivity with decreasing porosity was anticipated, since rock with greater porosity has reduced grain to grain contact per unit area conducting heat energy.

In essence, according as the rock porosity increases so too does the heat conductivity/convection through a 'porous area', which has a thermal conductivity value significantly less than that of rock (air = 0.024 W/mK, water = 0.58 W/mK (Coté and Konrad, 2005)), thereby diminishing the bulk thermal conductivity of the rock mass. These results are typical of those found by previous researchers, with the porosity of rock deemed to be a major contributory factor in the thermal conductivity

of various rock types. Furthermore the degree of saturation of these pores has a notable effect on the thermal conductivity, as highlighted by the results of the varying moisture contents in Figure 5.

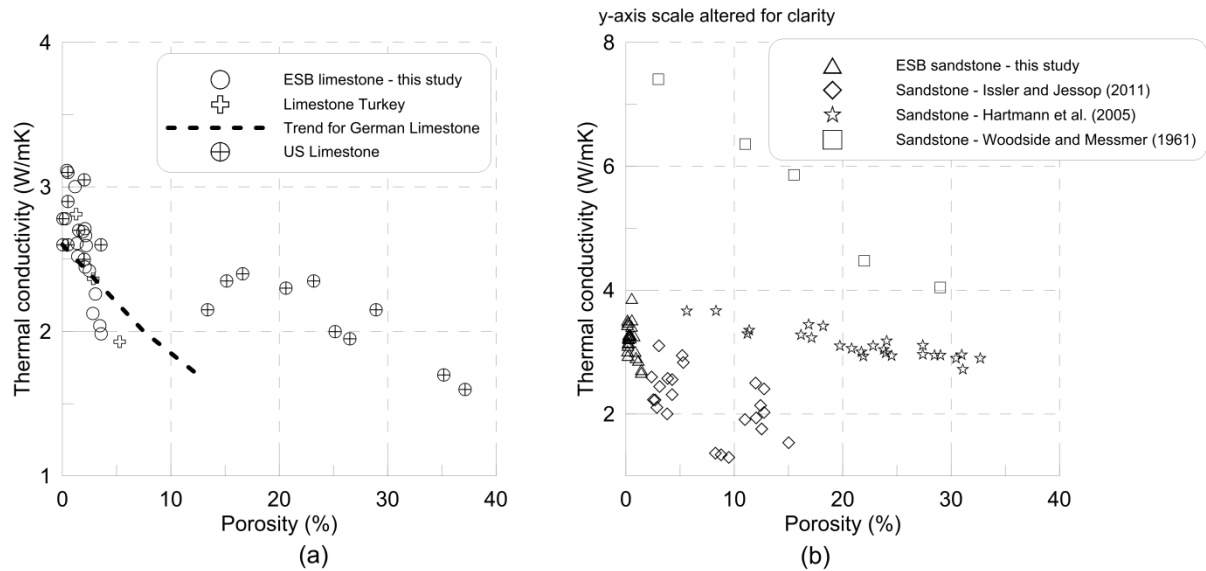


Figure 7 Comparison of thermal conductivity vs porosity against results of previous researchers for (a) limestone and (b) sandstone samples

A plot of the thermal conductivity values against the corresponding bulk density values for both the limestone and sandstone samples are presented in Figure 8. In both instances there does not appear to be a relationship between thermal conductivity and density. As expected factors such as porosity and mineral composition have a more prominent effect of the thermal conductivity of the rock mass. The notable scatter of density results for both rock types highlights the diversity of densities, which is typical of sedimentary rocks attributable to the formation of the rocks from various grains and minerals.

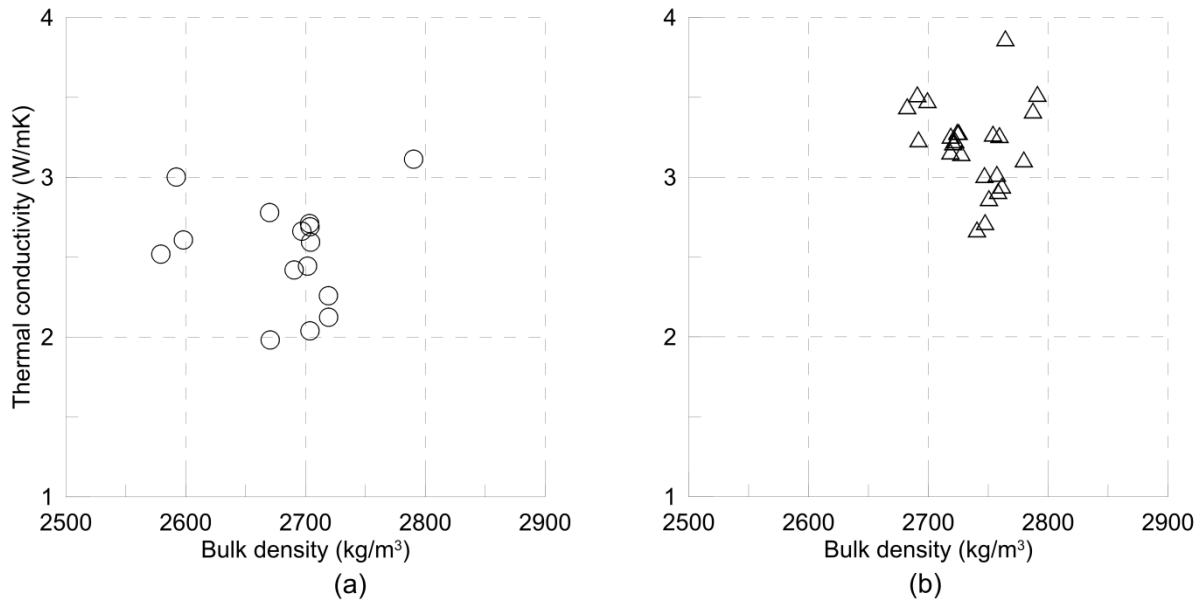


Figure 8 Thermal conductivity vs. density for (a) Calp limestone and (b) sandstone

5.2 Supplementary testing with the UCD Divided Bar Apparatus

Granite and schist samples were obtained from the Geological Survey of Ireland and were tested for thermal conductivity only owing to the small number of samples, with the results reported in Table 4. These samples were tested to evaluate the reliability of the UCD divided bar apparatus when measuring different rock types with thermal conductivity values atypical to those of the limestone and sandstone. Both the granite and schist samples were tested as received without saturation, therefore it is expected that the attained results are less than the potential maximum value of thermal conductivity. The granite had an average thermal conductivity value of 2.43 W/mK which lies within the range of 2.8 ± 0.6 W/mK as reported by Barker (1996), whilst the schist averaged out at 4.65 W/mK which is within the range of 4.1 – 6.8 W/mK as reported by Clark and Niblett (1956). The values received by the UCD divided bar apparatus in Table 4 are compared to those reported in the data library of EED (2010), which is one of the most common software programs used for geothermal energy design. The average thermal conductivity values acquired by the UCD divided bar apparatus for granite, limestone and sandstone lie within the range of values reported by EED, however there were no values for schist within the EED data library.

Material	EED Library of Standard λ (W/mK) values			UCD Average
	Minimum	Recommended	Maximum	
Granite	2.10	3.40	4.07	2.43
Limestone	1.96	2.20	2.78	2.59
Sandstone	1.28	2.30	5.10	3.21
Schist	n/a	n/a	n/a	4.65

Table 4. Comparison with Thermal Conductivity values from EED 2010

5.3 Photographic Analysis of samples tested on the UCD Divided Bar Apparatus

Further evaluation of the rock discs tested on the UCD divided bar apparatus included photographing a select number of samples under a Nikon Eclipse polarizing microscope at the UCD Geology laboratory, in an attempt to understand the difference in microscopic structure and mineralogy between the different rock types. Four of these photographic records are displayed in Figure 9 and Figure 10. Only one of each rock type was photographed, as variance in mineral structure with depth would not be evident. Figure 9 shows a photograph of (a) sandstone from a depth of 369 m b.g.l and (b) Calp limestone from a depth of 116 m b.g.l., with the line on both photographs represents a distance of 200 μm .

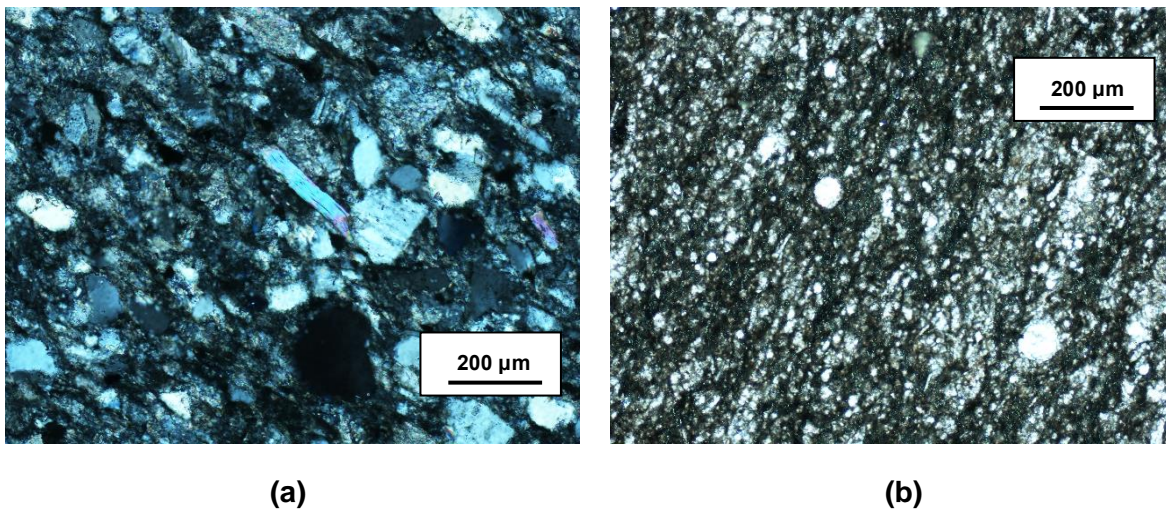


Figure 9 Microscope photos of (a) sandstone and (b) Calp limestone

The Calp limestone consists of dark grey massive limestones, shaley limestones, and massive mudstones. Evidently the limestone is comprised of a variety of different materials and minerals including very fine clay minerals and the occasional fossil or shell as can be seen by the white 'dots' in the photograph. As expected the sandstone exhibits coarser grain sizes in relation to the Calp limestone. Supplementary to the photographing, samples were also examined under a scanning electron microscope to establish what the constituent minerals of the rock samples were. The main mineral in the limestone is calcium carbonate with the inclusion of clay minerals also such as mica and feldspar. Minerals in the sandstone include silicon dioxide, calcium carbonate and some quartz showing up white in the photograph. It is most likely that the existence of quartz minerals ($\lambda = 7.69 \text{ W/mK}$, (Coté and Konrad, 2013)) coupled with larger grain sizes are the dominant contributory factors towards the higher thermal conductivity values of the sandstone samples relative to the limestone samples.

Figure 10 shows (a) granite sample tested and (b) the schist sample tested on the UCD divided bar apparatus, again with the line representing a distance of 200 μm .

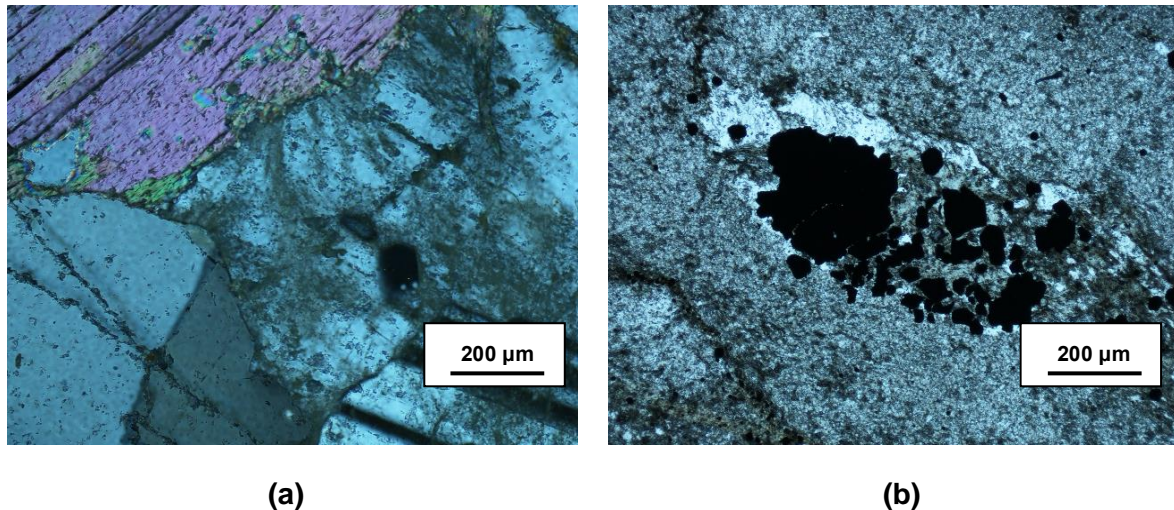


Figure 10 Microscope photos of (a) Granite and (b) Schist

It is immediately apparent that the mineral sizes of the granite and schist are much larger than those of the limestone and sandstone. The main constituent minerals of the granite samples are mica, quartz and feldspar, whilst the dominant minerals in the schist include calcium carbonate, sulphide and pyrite. The presence of greater quantities of quartz minerals within granite, in addition to larger grain sizes constitutes the main reasons why granite should have a greater thermal conductivity

value than limestone and sandstone. However the values attained here are broadly similar to the sandstone and limestone, as a result of the samples not being saturated prior to testing. The schist samples yielded the highest values of thermal conductivity measured in the UCD divided bar apparatus thus far, owing to the presence of pyrite minerals which have a thermal conductivity value of 19.2 W/mK (Horai, 1971).

5.4 Validation of Test Results from the UCD Divided Bar Apparatus

Upon completion of all scheduled testing it was decided to perform some auxiliary testing with the UCD divided bar apparatus, in an attempt to ascertain if the results obtained from various tests could be repeated. Samples chosen to examine for repeatability on the divided bar included the three granite samples previously tested along with some arbitrary 35 mm diameter core pieces. The results of these tests are compiled in Table 5, which includes the two different test results and their associated percentage difference.

Sample Number	First Test λ (W/mK)	Second Test λ (W/mK)	% Difference
NR – 12	1.40	1.33	5
NR – 33	1.94	1.93	1
NR – 47	1.35	1.26	7
NR – 64	1.35	1.33	2
NR – 70	1.25	1.26	1
Granite 1	2.65	2.54	4
Granite 2	2.25	2.33	3
Granite 3	2.40	2.37	2

Table 5. Repeatability of tests on the UCD divided bar apparatus

The highest percentage difference in test results was 7% with an average percentage difference of 3% for the eight tests. Reports from commercially used divided bars generally have a variance of 2 – 5% for repeated tests, thus affirming the competence of the UCD divided bar as an effective thermal conductivity measuring device. It is anticipated that the repeatability of the UCD divided bar

apparatus will be further confirmed by comparing conductivity measurements on a range of materials of differing conductivity against measurements made by a number of other laboratories. Further to the repeatability, two samples of the Calp limestone were tested with the UCD thermal needle probe (Hemmingway and Long, 2012b). The probe system includes the TP02 'Non-Steady-State Probe for Thermal Conductivity Measurement', with a large length to diameter ratio (150 mm / 1.5 mm). Utilisation of the needle probe for testing rock samples proved difficult as a result of having to predrill a relatively small diameter hole to a depth of 150mm and backfill with a contact material.

The value obtained using the probe for the range 74.0 – 74.52 m b.g.l was 2.67 W/mK and the value obtained at 95.0 – 95.66 m b.g.l was 2.53 W/mK as shown in Table 6. In both instances the results from the thermal probe tests are approximately 5 % greater than the corresponding average divided bar value, which is a favourable result with regards to validation of the UCD divided bar results. The needle probe test measures thermal conductivity over a depth of approximately 150 mm, whereas the divided bar apparatus measures discs of 20 mm, and in addition the needle probe measures radial conductivity, while the divided bar measures axial conductivity. The two can be significantly different in layered rocks, with axial thermal conductivity generally lower than radial thermal conductivity. Therefore the observed variance in the corresponding results is to be expected.

Sample Range (m bgl)	λ Divided bar (W/mK)				λ Needle Probe (W/mK)
	A	B	C	A_v	
Calp 74.000 – 74.520	2.26	2.76	2.61	2.54	2.67
Calp 95.000 – 95.660	2.55	2.40	2.23	2.39	2.53

Table 6. Comparison between divided bar & needle probe results

6. Conclusions

One of the most challenging aspects facing engineers designing a borehole heat exchanger is an accurate assessment of the ground parameters, including the

thermal conductivity, of the surrounding ground. The primary objective of this research was to develop a method for measuring the thermal conductivity of rock within the laboratory in an uncomplicated and economical manner, allowing for continuity of use. Testing the thermal conductivity of rock samples in the UCD laboratory was achieved by means of a steady-state divided bar apparatus designed and developed as part of this research. The total cost of the UCD divided bar apparatus was €2,170 which compares favourably with the cheapest commercial equivalent on the market which costs approximately €12,000.

Rock samples tested on the UCD divided bar apparatus included Calp limestone and sandstone, with some granite and schist introducing variety to the samples tested. In addition to testing the thermal conductivity of the rock samples, parameters such as density, porosity and moisture content were also determined. Finally thin sections were made from the tested rock cores, allowing photographic analysis and an appraisal of the mineral composition. The values of thermal conductivity obtained from the test samples in this study ranged from 1.98 – 3.87 W/mK which are consistent with the expected values of limestone and sandstone. Rocks are, as a rule, poor conductors of heat and have a comparatively narrow range values of thermal conductivity values (0.1 - 7 W/mK), which agrees with the values obtained in this study.

From analysis of the test results it can be concluded that the most important factors controlling the thermal conductivity of the rock samples, are mineral composition and the degree of porosity. There was little or no correlation observed between density and depth with thermal conductivity. In summary the UCD divided bar apparatus is deemed to be an acceptable means of measuring the thermal conductivity of rock in the laboratory from the following attainments:

- (i) Comparable results to those published by previous researchers.
- (ii) Validation of divided bar test results by means of a thermal needle probe.
- (iii) Satisfactory level of repeatability with different diameter and rock test samples.

References

- BARKER, C. 1996. Thermal Modeling of Petroleum Generation: Theory and Applications. *Amsterdam: Elsevier*.
- BEARDSMORE, G. R. & CULL, J. P. 2001. *Crustal Heat Flow: A Guide to Measurement and Modelling*, CAMBRIDGE UNIVERSITY PRESS.
- BIRCH, F. & CLARK, H. 1940. The Thermal Conductivity of Rocks and Its Dependence upon Temperature and Composition. *American Journal of Science*.
- CANAKCI, H., DEMIRBOGA, R., KARAKOC, B. & SIRIN, O. 2007a. Thermal conductivity of limestone from Gaziantep (Turkey). *Building and Environment*, 42, 1777-1782.
- CANAKCI, H., DEMIRBOGA, R., KARAKOC, M. B. & SIRIN, O. 2007b. Thermal conductivity of limestone from Gaziantep (Turkey). *Building and Environment*, 42, 1777-1782.
- CHO, W. J., KWON, S. & CHOI, J. W. 2009. The thermal conductivity for granite with various water contents. *Engineering Geology*, 107, 167 -171.
- CLARK, S. P. & NIBLETT, E. R. 1956. Terrestrial heat flow in the Swiss Alps: Monthly Notices. *Royal Astronomical Society Geophysical Supplement*, 7, 176 - 195.
- COTÉ, J. & KONRAD, J. 2005. A generalized thermal conductivity model for soils and construction materials. *Canadian Geotechnical Journal*, 42, 443-458.
- COTÉ, J. & KONRAD, J. 2013. Thermal conductivity of base-course materials. *Canadian Journal of Civil Engineering*, 40(2), 172-180.
- EED 2010. Energy Earth Designer Ver.3.16. *Blocon Sweden, Nordmannavagen 96, SE-224 74*.
- GRÖSCHEL-BECKER, H. M., DAVIS, E. E. & FRANKLIN, J. M. 1994. Physical Properties Of Massive Sulfide From Site 856, Middle Valley, Northern Juan De Fuca Ridge. *Proceedings of the Ocean Drilling Program, Scientific Results*, Vol 139.
- HARTMANN, A., RATH, V. & CLAUSER, C. 2005. Thermal conductivity from core and well log data. *International Journal of Rock Mechanics & Mining Services*, Vol 42, 1042 - 1055.
- HEMMINGWAY, P. & LONG, M. 2012a. Design and Development of a Low-Cost Thermal Response Rig. *Proceedings of the Institution of Civil Engineers - Energy*, 165(EN3), 137-148
- HEMMINGWAY, P. & LONG, M. 2012b. Interpretation of in situ and laboratory thermal measurements resulting in accurate thermogeological

characterization. In: TAYLOR & FRANCIS GROUP, L. (ed.) *Geotechnical and Geophysical Site Characterization 4. Brazil*.

HORAI, K. 1971. Thermal conductivity of rock-forming minerals. *Journal of Geophysical Research*, 76, 1278-1308.

ISSLER, D. & JESSOP, A. 2011a. Thermal Conductivity Analysis of Cenozoic, Mesozoic and Paleozoic Core Samples, Beaufort-Mackenzie Basin, Northern Canada. *Geological Survey of Canada*, Open File 6734, 128p.

ISSLER, D. R. & JESSOP, A. M. 2011b. Geological Survey of Canada open file 6734. *Thermal conductivity analysis of Cenozoic, Mesozoic and Paleozoic core samples, Beaufort-Mackenzie Basin, northern Canada*

JONES, M. Q. W. 2003. Thermal properties of stratified rocks from Witwatersrand gold mining areas. *The Journal of The South African Institute of Mining and Metallurgy*.

LIDE, D. 2009. *CRC handbook of chemistry and physics : a ready-reference book of chemical and physical data*

PECHNIG, R., MOTTAGHY, D., KOCH, A., JORAND, R. & CLAUSER, C. 2007. Prediction of thermal properties for Mesozoic rocks of Southern Germany. *Proceedings of the European Geothermal Congress, Unterhaching, Germany*, 1-4.

POPOV, Y., PRIBNOW, D. F. C., SASS, J. H., WILLIAMS, C. F. & BURKHARD, H. 1999. Characterization of rock thermal conductivity by high-resolution optical scanning *Geothermics* 28, 253-276

ROBERTSON, E. 1988. Thermal properties of rocks. *United States Geological Survey Open File Report 88-441. Reston, Virginia*.

RPA 2008. Dublin Metro North Geotechnical Data Report. Railway Procurment Agency.

SIBBITT, W. L., DODSON, J. G. & TESTER, J. W. Thermal conductivity of rocks associated with energy extraction from hot dry rock geothermal systems 15th International Thermal Conference Proceedings, 1979.

STEPANIC, N. & MILOSEVIC, N. 2009. Correction of the influence of thermal contact resistance in thermal conductivity measurements using the guarded hot plate method. *Serbian Journal of Electrical Engineering*, 6 (3), 479-488.

ULUSAY, R. & HUDSON, J. A. 2007. *The complete ISRM Suggested methods for rock characterization, testing and monitoring: 1974 - 2006*, ISRM Turkey.

WOODSIDE, W. & MESSMER, J. 1961. Thermal conductivity of porous media. *Journal of Applied Physics*, 32, 1699-1706.

